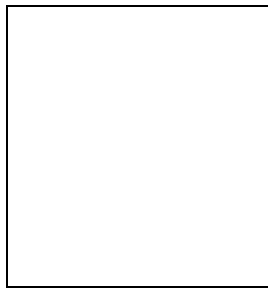


Consilience of High- T_c Theories

J. B. Marston

Department of Physics, Brown University, Providence, Rhode Island 02912-1843 USA



Improvements both in the quality and in the variety of experiments on high-temperature superconductors have yielded new insights into the microscopic origins of pairing. A number of competing theories have already been ruled out. Some of the more promising descriptions – gauge theories, coupled-chains, nesting instabilities, nodal liquids, and stripes – share features in common. A unified picture of the cuprates is beginning to emerge.

1 Introduction

In his recent book *Consilience: The Unity of Knowledge*, biologist E. O. Wilson reintroduced the word “consilience” into the English language. William Whewell wrote in 1840 that “The Consilience of Induction takes place when an Induction, obtained from one class of facts, coincides with an Induction, obtained from another different class. This Consilience is a test of the truth of the Theory in which it occurs¹. ” The cuprate high temperature superconductors are complex enough that it is appropriate to apply this truth principle to sort out various models. In this brief overview, I focus on *some* of the theories which have at least a chance of surviving. I will argue that recent years have seen a consilience, a coming-together, of theories of high temperature superconductivity.

This lecture was presented in Hanoi at the *International Workshop on Superconductivity, Magneto-Resistive Materials, and Strongly Correlated Quantum Systems*. Vietnam is a country with a long tradition of Buddhism. It is therefore fitting to recall the second of Buddhism’s Four Noble Truths: Attachment leads to suffering. It is important to not become too attached to any one theory of high-temperature superconductivity! Some are completely wrong; others mix strong and weak features, and none are as yet definitive.

2 Key Experiments

Recent experimental advances show that the various high temperature superconductors share much in common. A good overview of the cuprate materials and their key experimental properties can be found in a recent review by Maple². Experiments now agree that there is $d_{x^2-y^2}$ superconducting order³, at least in the hole-doped compounds. One of the most intriguing phenomena is the existence of a pseudogap in the density of states at temperatures *above* the superconducting transition temperature T_c . Many experiments show, or are at least consistent with, the existence of the pseudogap^{4,5,6,7,8}. Four other key experimental results are:

1. Rough Electron-Hole Symmetry: As emphasized by Maple², the behavior of the electron doped materials, such as $Nd_{2-x}Ce_xCuO_{4-y}$, is qualitatively similar to that of the hole-doped compounds such as $La_{2-x}Sr_xCuO_{4-y}$. In particular, both are antiferromagnetic insulators at small x which become superconducting at larger values of x . Whether or not the electron doped materials are d-wave superconductors is a crucial question. If they are s-wave, much of the subsequent discussion in this article is falsified, or at the very least must be reworked.

2. Angle Resolved Photoemission (ARPES): Although ARPES experiments continue to contradict each other^{9,10,11}, some features stand out. Nesting of the Fermi surface seems to have been observed¹². And one insulating antiferromagnetic parent compound shows a very interesting electron dispersion¹³, similar to that of a d-wave superconductor, despite the absence of superconductivity, see Sec. 4 below.

3. Neutron Scattering: Neutrons are sensitive to both static and fluctuating magnetic moments. A useful summary is presented by Mason¹⁴. Incommensurate magnetic fluctuations have been observed for some time in doped 214 compounds^{15,16,17,18}, and the deviation of the peak wavevectors from the Néel ordering wavevector $\vec{Q} = (\pi, \pi)$ is proportional to the doping. The recent observation of similar incommensurate peaks in the 123 material¹⁹ suggests that this behavior is common, and perhaps universal, to the cuprates.

4. Phase Separation and Stripes: Although phase separation into *static* stripes may occur only in some of the cuprates^{20,21}, and at special dopings such as $x = 1/8$, there is mounting evidence for ubiquitous, but slowly shifting stripes, in particular from ^{63}Cu NQR measurements²². Even when there is no true long-range stripe order, the stripe dynamics may be slow enough that the stripes can be treated for most purposes as static.

3 Hubbard and Related Models

Anderson's early insight was that the Hubbard model is a good starting point for theories of cuprate superconductivity²³. The one-band model,

$$H = -t \sum_{\langle \mathbf{x}, \mathbf{y} \rangle} (c_{\mathbf{x}}^{\dagger\alpha} c_{\mathbf{y}\alpha} + H.c.) + U \sum_{\mathbf{x}} (c_{\mathbf{x}}^{\dagger\alpha} c_{\mathbf{x}\alpha} - 1)^2 , \quad (1)$$

can be justified starting from the more complete three-band model which describes the $p_{x,y}$ oxygen orbitals as well as the $d_{x^2-y^2}$ orbitals of the copper atoms²⁴. For simplicity only nearest-neighbor hopping, and on-site Coulomb repulsion, appear in the above Hamiltonian; however, next-nearest neighbor hopping can be important. Furthermore, the assumption that the inverse-square Coulomb interaction is screened down to a pure on-site repulsion certainly breaks down if there is phase separation (see Sec. 5).

At half-filling, and on a square lattice, nesting instabilities open up a charge gap and the system becomes an antiferromagnetic insulator. The low energy spin degrees of freedom can be described in terms of the electron operators as:

$$\vec{S}_{\mathbf{x}} = \frac{1}{2} c_{\mathbf{x}}^{\dagger\alpha} \vec{\sigma}_{\alpha}^{\beta} c_{\mathbf{x}\beta} \quad (2)$$

subject to the constraint

$$n_{\mathbf{x}} \equiv c_{\mathbf{x}}^{\dagger\alpha} c_{\mathbf{x}\alpha} = 1 . \quad (3)$$

The representation of the spins in terms of the underlying fermions is not as economical as the representation of the spins themselves, since the spin operators of Eq. 2 are invariant under $U(1)$ gauge transformations at each lattice point^{25,26}

$$\begin{aligned} c_{\mathbf{x}\alpha} &\rightarrow e^{i\theta_{\mathbf{x}}} c_{\mathbf{x}\alpha} \\ c_{\mathbf{x}}^{\dagger\alpha} &\rightarrow e^{-i\theta_{\mathbf{x}}} c_{\mathbf{x}}^{\dagger\alpha} \end{aligned} \quad (4)$$

because the local phase rotation $\theta_{\mathbf{x}}$ cancels out. We denote this infinite gauge symmetry $U(1)_x^\infty$. The physical meaning of this local symmetry is simply that the charge degrees of freedom are frozen out and play no role in the insulating magnet. The underlying fermions have both charge and spin degrees of freedom, but as the number of fermions on each site is fixed to be one, only the spin degree of freedom is active.

Conversely, in the $U \rightarrow 0$ limit, the Hubbard model reduces to a non-interacting tight-binding model

$$H = -t \sum_{\langle \mathbf{x}, \mathbf{y} \rangle} c_{\mathbf{x}}^{\dagger\alpha} c_{\mathbf{y}\alpha} + H.c. \quad (5)$$

which is clearly not invariant under the $U(1)_x^\infty$ transformations, Eq. 4. Distinct $U(1)$ rotation angles at neighboring sites, θ_x and θ_y do not cancel out. Physically this just means that the electron number is not conserved as the electrons hop from site to site. However, in momentum space,

$$H = \sum_{\mathbf{k}} \epsilon_{\mathbf{k}} c_{\mathbf{k}}^{\dagger\alpha} c_{\mathbf{k}\alpha}; \quad \epsilon_{\mathbf{k}} = -2t[\cos(k_x) + \cos(k_y)] . \quad (6)$$

The Hamiltonian is instead invariant under a different infinity of $U(1)$ rotations²⁷, now at each point in momentum space, rather than position space:

$$\begin{aligned} c_{\mathbf{k}\alpha} &\rightarrow e^{i\theta_{\mathbf{k}}} c_{\mathbf{k}\alpha} \\ c_{\mathbf{k}}^{\dagger\alpha} &\rightarrow e^{-i\theta_{\mathbf{k}}} c_{\mathbf{k}}^{\dagger\alpha} . \end{aligned} \quad (7)$$

This $U(1)_k^\infty$ symmetry, like the $U(1)_x^\infty$ symmetry explored above, has a clear physical interpretation: in the absence of interactions and disorder, momentum is a good quantum number for the single-particle states, as these are infinitely long-lived. In summary,

$$\begin{aligned} U(1)_x^\infty &\leftrightarrow \text{insulating solid} \\ U(1)_k^\infty &\leftrightarrow \text{conducting liquid.} \end{aligned} \quad (8)$$

The real cuprates lie somewhere between these two extreme limits, and it is the tension between these two limits that leads to much interesting physics.

Further progress can be made by noting that $U \gg t$; hence, double-occupied sites are energetically disfavored in hole-doped compounds. We can enforce this reduction of the on-site Hilbert space from 4 states to 3 by employing slave bosons to represent the holes and write the t-J model²⁴ as follows:

$$H = -t \sum_{\langle \mathbf{x}, \mathbf{y} \rangle} (c_{\mathbf{x}}^{\dagger\alpha} b_{\mathbf{x}} c_{\mathbf{y}\alpha} b_{\mathbf{y}}^\dagger + H.c.) + J \sum_{\langle \mathbf{x}, \mathbf{y} \rangle} (\vec{S}_{\mathbf{x}} \cdot \vec{S}_{\mathbf{y}} - \frac{1}{4} n_{\mathbf{x}} n_{\mathbf{y}}) . \quad (9)$$

Every time an electron c hops from site \mathbf{x} to \mathbf{y} , a hole b hops in the reverse direction. The holonomic constraint $c_{\mathbf{x}}^{\dagger\alpha} c_{\mathbf{x}\alpha} + b_{\mathbf{x}}^\dagger b_{\mathbf{x}} = 1$ then forces the total electron number on each site to be equal to zero or one, but not two.

There are many approximate solutions of the t-J model. In the following sections I describe several different starting points which, surprisingly, lead to rather similar conclusions.

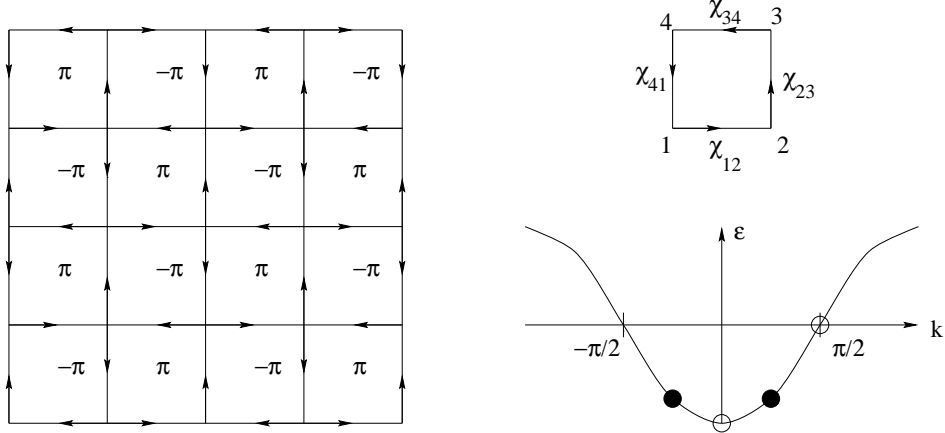


Figure 1: Orientation of the χ_{xy} fields in the π -flux phase. Since $-\pi$ flux is equivalent to π flux, this phase has the full translational symmetry of the underlying lattice and respects time-reversal symmetry. By considering a single plaquette of just four sites, it is clear that $\pm\pi$ flux is energetically favored as the filled electronic states have lower net energy (solid dots) compared to zero flux (open dots).

4 Mean-Field and Gauge Theories of the Undoped Antiferromagnet

The first starting point I consider is a systematic solution of the $t - J$ model by means of a $1/N$ expansion^{26,28}. The basic idea is to generalize the usual two types of spin, up and down, to N types, and solve the resulting $SU(N)$ t-J model in the $N \rightarrow \infty$ limit. Fluctuations disappear in the $N \rightarrow \infty$ limit and complex-valued mean-fields along the bonds acquire expectation values:

$$\chi_{xy} = \frac{J}{N} c_x^\dagger c_y^\alpha . \quad (10)$$

An additional set of scalar fields, $\phi_x(t)$, are introduced as Lagrange multipliers to enforce the holonomic constraint on the occupancy. Under the local $U(1)$ gauge transformations, Eq. 4, the χ fields transform like the spatial link variables of a compact lattice gauge theory, while the ϕ fields transform as the time-component of the gauge fields:

$$\begin{aligned} \chi_{xy}(t) &\rightarrow e^{i[\theta_y(t) - \theta_x(t)]} \chi_{xy}(t) \\ \phi_x(t) &\rightarrow \phi_x(t) + \frac{d\theta_x(t)}{dt} . \end{aligned} \quad (11)$$

One annoying problem with the large- N limit is that, close to half-filling, the lowest-energy solution is dimerized: χ_{xy} is non-zero only on disconnected bonds. This solution, which is unphysical, can be eliminated by the introduction of biquadratic spin-spin interactions²⁸ which do nothing to the original $SU(2)$ model (as they reduce to the usual bilinear exchange at $N = 2$) but which suppress dimerization for $N > 2$. Furthermore, instantons do not induce dimerization as they do in the bosonic $SU(N)$ and $Sp(N)$ formulations²⁹. This is clearly demonstrated by an exact solution which shows no dimerization³⁰.

At half-filling the ground state is the π -flux phase^{26,31}. The flux is defined by the gauge invariant plaquette operator $\langle \chi_{12}\chi_{23}\chi_{34}\chi_{41} \rangle < 0$ with the χ fields oriented as shown in Fig. 1. Rokhsar pointed out³² a simple way to see that non-zero flux is energetically favored: it lowers the kinetic energy of the fermions on the lattice, an effect which is particularly easy to see for the four-site problem, see Fig. 1. The spectrum is markedly different from that of a tight-binding model as now the fermion dispersion has the form:

$$\epsilon(\vec{k}) \propto \pm \sqrt{\cos^2(k_x) + \cos^2(k_y)} . \quad (12)$$

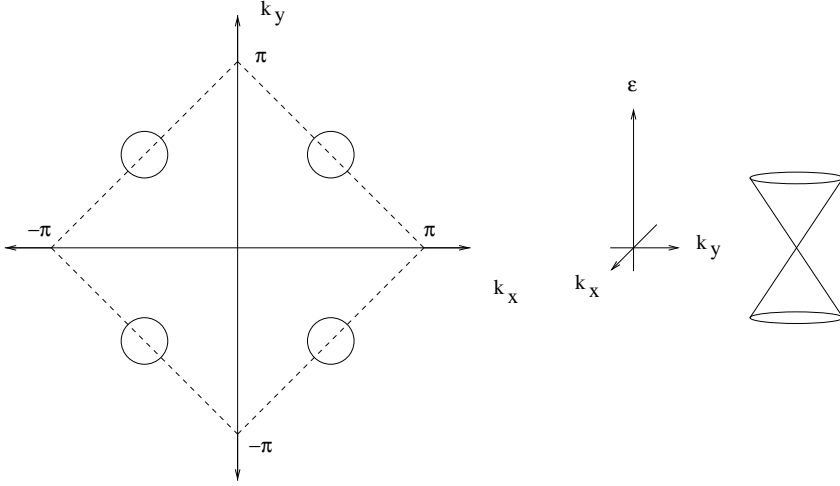


Figure 2: Dispersion of the flux phase. There is a pseudo-gap everywhere except at the nodal points $\vec{k} = (\pm\pi/2, \pm\pi/2)$. These points are paired and the dispersion is linear (cone) like that of massless Dirac fermions.

The negative energy states are filled, and the nesting instability has been removed by the appearance of a pseudogap everywhere except at the discrete points $\vec{k} = (\pm\pi/2, \pm\pi/2)$ where the density of states vanishes linearly as shown in Fig. 2. It is remarkable that precisely this dispersion is seen in ARPES experiments¹³ on the insulating parent compound $\text{Ca}_2\text{CuO}_2\text{Cl}_2$, an observation emphasized by Laughlin³³.

Because the mean-fields χ and ϕ are singlets under $SU(N)$ spin rotations, long-range spin-order is impossible in the $N \rightarrow \infty$ limit. To recover Néel order requires the consideration of non-perturbative $1/N$ corrections – a notoriously difficult problem. Some progress^{34,35} was made by recognizing that formation of the long-range spin order is equivalent to the dynamical generation of fermion mass³⁴ in $2 + 1$ dimensional $U(1)$ gauge theory, a problem that has been studied by particle theorists. At large- N there is a global $SU(2N)$ symmetry which combines the N spin species with the two types of gapless points in the reduced Brillouin zone at $\vec{k} = (\pm\pi/2, \pi/2)$. This symmetry breaks down at finite- N as $SU(2N) \rightarrow SU(N) \otimes SU(N)$ when the fermions become gapped. Other massless excitations then arise, which can be identified as the Goldstone modes or spin-waves of the Néel ordered magnetic state, or equivalently as bound states of particles and holes, otherwise known as mesons.

An interesting analysis of $1/N$ corrections to the $U \rightarrow \infty$ Hubbard model, with no spin exchange interaction J , has recently been carried out³⁶. At leading order, as expected, the system is a Fermi liquid for any doping away from half-filling. However, by working to order $1/N$ and then setting $N = 2$, Fermi liquid behavior is found to be destabilized at light doping $x < 0.07$, in rough agreement with the large- N results for the $t - J$ model.

5 Phase Separation at Non-Zero Doping and Incommensurate Order

At non-zero doping there is the possibility of a staggered flux phase (SFP). In the SFP the hole occupancy is assumed to be uniform, $\langle b_x^\dagger b_x \rangle = Nx/2$, and the flux is reduced in magnitude from π , eventually disappearing altogether at large enough doping. Time-reversal and translational symmetries are broken in the SFP and orbital currents with real magnetic fields arise. These appear to be ruled out experimentally³⁷.

On the other hand, phase separation into stripes had been predicted on theoretical grounds³⁸, prior to any clear experimental observation of the phenomenon. The stability of stripes depends on the size of the hopping matrix elements beyond nearest-neighbor exchange³⁹. Phase separation solves the problem of the breaking of time-reversal and translational symmetries in the SFP.

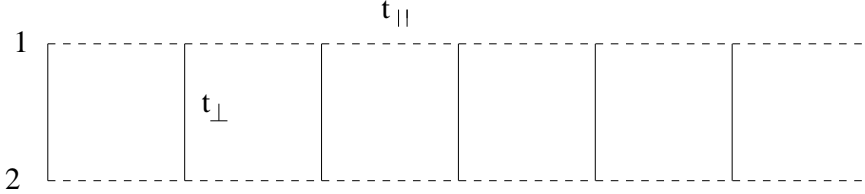


Figure 3: A ladder consisting of two coupled Hubbard chains, numbered 1 and 2, with intrachain hopping in the x-direction, t_{\parallel} , and interchain hopping in the y-direction, t_{\perp} .

Phase separation into stripes also can explain the incommensurate, and nearly critical¹⁵, spin fluctuations seen in neutron scattering experiments in the 214 compound¹⁶ and recently in the 123 material¹⁹. The two problems are solved simultaneously by assuming that the electron-rich region is an antiferromagnetic insulator described by the π -flux phase, with its strong tendencies towards spin ordering. The infrared divergences³⁴ at finite- N are cut-off by the limited size of the electron-rich region. Incommensurate spin peaks arise due to these finite-size effects. The tendency to phase separate can also be viewed fruitfully⁴⁰ in terms of a Fermi liquid close to a quantum critical point (QCP).

6 Squares, Chains, and Ladders

Another way to study the behavior of the t-J model on the square lattice is to build up the lattice systematically from smaller subunits. For example, the four site system, a square plaquette, can be easily diagonalized. At half-filling, the spin-spin correlations in the ground state are such that the expectation value of the plaquette operator has a negative value. To be precise, in the physical $N = 2$ case, the expectation values of three-spin operators such as $\langle \vec{S}_1 \cdot (\vec{S}_2 \times \vec{S}_3) \rangle$ vanish if there is no time-reversal symmetry breaking, and

$$\begin{aligned} \langle \chi_{12} \chi_{23} \chi_{34} \chi_{41} \rangle &= \frac{J^4}{16} \left\{ \frac{1}{8} + \frac{1}{2} [\langle \vec{S}_2 \cdot \vec{S}_3 \rangle + \langle \vec{S}_2 \cdot \vec{S}_4 \rangle + \langle \vec{S}_3 \cdot \vec{S}_4 \rangle - \langle \vec{S}_1 \cdot \vec{S}_2 \rangle - \langle \vec{S}_1 \cdot \vec{S}_3 \rangle - \langle \vec{S}_1 \cdot \vec{S}_4 \rangle] \right. \\ &\quad \left. - 2 [\langle (\vec{S}_1 \cdot \vec{S}_2)(\vec{S}_3 \cdot \vec{S}_4) \rangle + \langle (\vec{S}_1 \cdot \vec{S}_4)(\vec{S}_2 \cdot \vec{S}_3) \rangle - \langle (\vec{S}_1 \cdot \vec{S}_3)(\vec{S}_2 \cdot \vec{S}_4) \rangle] \right\} < 0. \quad (13) \end{aligned}$$

Thus flux π penetrates the plaquette. The same result holds for the 4×4 lattice with periodic boundary conditions⁴¹ providing added support for the flux phase.

The square lattice can also be built up chain-by-chain. A single Hubbard chain, with repulsive interactions, is a Luttinger liquid away from half-filling; at half-filling a gap develops in the charge sector, while the spin sector remains gapless in accord with the physics of a spin-1/2 quantum antiferromagnetic chain. S-wave Cooper pairing is inhibited by the strong on-site repulsion and there can be no d-wave superconducting tendencies along a single chain.

Coupling two such chains with transverse hopping t_{\perp} , as shown in Fig. 3, leads to more interesting possibilities. Following Fisher⁴² the first step is to diagonalize the $U = 0$ problem by introducing bonding ($k_y = 0$) and anti-bonding ($k_y = \pi$) orbitals:

$$\begin{aligned} k_y = 0 : \quad b_{x\alpha} &\equiv \frac{1}{\sqrt{2}} [c_{x\alpha 1} + c_{x\alpha 2}], \quad \epsilon_{k_x} = -2t_{\parallel} \cos(k_x) - t_{\perp} \\ k_y = \pi : \quad a_{x\alpha} &\equiv \frac{1}{\sqrt{2}} [c_{x\alpha 1} - c_{x\alpha 2}], \quad \epsilon_{k_x} = -2t_{\parallel} \cos(k_x) + t_{\perp}. \end{aligned} \quad (14)$$

Now if the Hubbard repulsion is turned back on, the RG flows run away to large values suggesting that charge and spin gaps form and the problem should be studied from the strong-coupling viewpoint. Consider the limit $t_{\perp} \gg t_{\parallel}$, as it is clear that at half-filling spins on opposing sites

will pair into singlets because $J_{\perp} \approx 4t_{\perp}^2/U \gg J_{\parallel} \approx 4t_{\parallel}^2/U$. The ground state then may be written:

$$|\Psi_0\rangle = \prod_x \frac{1}{\sqrt{2}} [c_{x1}^{\dagger\uparrow} c_{x2}^{\dagger\downarrow} - c_{x1}^{\dagger\downarrow} c_{x2}^{\dagger\uparrow}] |0\rangle = \prod_x \frac{1}{\sqrt{2}} [b_x^{\dagger\uparrow} b_x^{\dagger\downarrow} - a_x^{\dagger\uparrow} a_x^{\dagger\downarrow}] |0\rangle. \quad (15)$$

Thus, although there is no true off-diagonal long-range order, there is a $d_{x^2-y^2}$ wave tendency because the last line looks like a Cooper-paired state with the sign of the pairing amplitude changing as k_y switches from 0 to π .

7 Nodal Liquid

A complementary approach to understanding the underdoped cuprates takes as its starting point the d-wave superconducting state^{43,44} with dispersion $\mathcal{E}(\vec{k})$ determined, using the tight-binding spectrum $\epsilon_{\vec{k}} \propto \cos(k_x) + \cos(k_y)$ and d-wave pairing gap function $\Delta_{\vec{k}} \propto \cos(k_x) - \cos(k_y)$, by the usual BCS calculation:

$$\mathcal{E}(\vec{k}) = \pm \sqrt{\epsilon_{\vec{k}}^2 + \Delta_{\vec{k}}^2} \propto \pm \sqrt{\cos^2(k_x) + \cos^2(k_y)}. \quad (16)$$

This “nodal liquid” theory, as its name suggests, focuses on the gapless nodal points at $\vec{k} = (\pm\pi/2, \pm\pi/2)$. As the doping is reduced a zero-temperature quantum phase transition to a non-superconducting, but pseudo-gapped, insulating state is envisioned. The “nodons,” or low-energy fermion quasiparticles near the nodes, carry the same quantum numbers as the fermions in the flux phase⁴³. Upon further reduction of the doping, antiferromagnetic order may arise⁴⁵.

8 Isotropic RG Analysis

The interplay between nesting, umklapp processes, and the formation of charge-density-wave (CDW), spin-density-wave (SDW), and BCS instabilities has been illustrated in a simple model of the Fermi surface which reduces the nested planes to just four Fermi points⁴⁶. In a recent paper, Furukawa and Rice use a generalized version of this model to argue that the spin gap in the cuprate superconductors can be understood as a consequence of umklapp processes⁴⁷. However, the whole Fermi surface can be retained. High-energy degrees of freedom are integrated out: In degenerate fermion systems this means that the inner and outer sides of the momentum shell which encloses the Fermi surface are shrunk successively⁴⁸. The RG flow can be investigated by multidimensional bosonization^{49,50}. The advantage of the bosonized RG calculation is that the existence of well-defined quasiparticles is not assumed *a priori*. Furthermore, interaction channels which possess $U(1)_k^{\infty}$ symmetry can be diagonalized exactly at the outset. Similar results have been obtained in the fermion basis^{51,52,53,54}.

Nested Fermi surfaces support many more low-energy scattering processes than circular Fermi surfaces⁵⁰. Some important processes are depicted in Fig. 4. Consequently, the quasiparticle lifetime $\tau \propto 1/T$ is much shorter than that in an ordinary Landau Fermi liquid ($\tau \propto 1/T^2$). Instead, the normal state is a marginal Fermi liquid and the agreement with transport data⁵⁵ is compelling.

The tendency towards spin-density order dominates all other instabilities close to half-filling. But slightly below half-filling, because nesting is not perfect but nonetheless effective, there is competition between the SDW and BCS instabilities. As the energy cutoff ϵ_c around the Fermi surface is reduced via the RG transformation towards ϵ_s , where ϵ_s is the energy deviation of the actual Fermi surface from perfect nesting, the SDW channel stops flowing but the BCS channel continues to renormalize logarithmically as its flow is independent of nesting. If the initial SDW coupling is small enough or if ϵ_s is large enough (the SDW channel does not develop an instability until $\epsilon_c \rightarrow \epsilon_s$) SDW order will not occur. Instead, d-wave superconductivity sets in at a sufficiently low temperature.

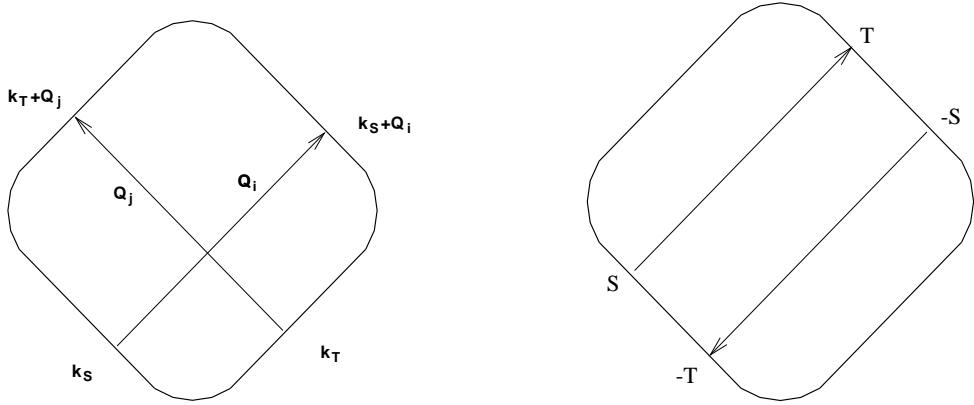


Figure 4: (a) A typical density-wave scattering channel which is permitted because $\mathbf{Q}_i + \mathbf{Q}_j$ is a reciprocal lattice wavevector. (b) A typical overlap between density-wave and BCS channels.

Table 1: Comparison of different theories.

Theory	Quantum Magnetism	Proximity to QCP(s)	$\vec{k} = (\pm\pi/2, \pm\pi/2)$
Gauge Theory	✓	✓	✓
Nodal Liquid	?	✓	✓
RG Analysis	✓	✓	✓
Stripes	✓	✓	This article
$SO(5)$	✓	✓	No

9 Consilience?

It should be noted that just about any theory which attempts to explain cuprate superconductivity in terms of an underlying electronic mechanism will favor d-wave order⁵⁶. More revealing is a comparison of other features of such theories. A summary of the four approaches discussed here, along with the more phenomenological $SO(5)$ theory of Zhang and collaborators⁵⁷ is presented in Table 1. Noted in the final column are theories with nodal excitations. It remains to be seen whether or not one unifying description will emerge from these pieces of the high- T_c puzzle.

Acknowledgments

I thank A. Houghton, H.-J. Kwon, C. Nayak and Z. Wang for recent helpful discussions. I would also like to thank the organizers of the *International Workshop* for their work in bringing the many foreign participants to Vietnam. This research was supported in part by the United States National Science Foundation under Grants Nos. DMR-9357613 and DMR-9712391.

References

1. As quoted by Edward O. Wilson in “Consilience: The Unity of Knowledge,” Alfred A. Knopf, Inc. (New York, New York, 1998).
2. M. Brian Maple, “High Temperature Superconductivity,” cond-mat/9802202.
3. H. Ding *et al.*, Phys. Rev. B **54**, 9678 (1996); C. C. Tsuei *et al.*, Nature **387**, 481 (1997); K. A. Kouznetsov *et al.*, Phys. Rev. Lett. **79**, 3050 (1997).
4. See, for instance, the table compiled by Robert F. Service, *Science*, **278**, 1879 (1997).

5. Guy Deutscher, *Nature* **397**, 410 (1999).
6. J. Corson *et al.* *Nature* **398**, 221 (1999); A. Millis, *Nature* **398**, 193 (1999).
7. R. S. Markiewicz and C. Kusko, “Comment on ‘Predominantly Superconducting Origin ...’ by N. Miyakawa *et al.*,” cond-mat/9810214.
8. C. Kusko and R. S. Markiewicz, “Remnant Fermi Surfaces in Photoemission,” cond-mat/9903317.
9. M. R. Norman *et al.*, *Nature* **392**, 157 (1998); M. R. Norman, “Fermi Surfaces, Fermi Patches and Fermi Arcs in High T_c Superconductors,” cond-mat/9904048.
10. A. Ino *et al.*, “Electronic Structure of $\text{La}_{2-x}\text{Sr}_x\text{CuO}_4$ in the Vicinity of Superconductor-Insulator Transition,” cond-mat/9902048.
11. Y.-D. Chuang *et al.*, “A Re-examination of the electronic structure of $\text{Bi}_2\text{Sr}_2\text{CaCu}_2\text{O}_{8+\delta}$ and $\text{Bi}_2\text{Sr}_2\text{Cu}_1\text{O}_{6+\delta}$ – An Electron-like Fermi Surface and the Absence of Flat Bands at E_F ,” cond-mat/9904050.
12. D. S. Dessau *et al.*, *Phys. Rev. Lett.* **71**, 2781 (1993); Z. X. Shen and D. S. Dessau, *Phys. Rep.* **253**, 1 (1995).
13. F. Ronning *et al.* *Science* **282**, 2067 (1998).
14. T. E. Mason, “Neutron Scattering Studies of Spin Fluctuations in High Temperature Superconductors,” cond-mat/9812287.
15. G. Aeppli *et al.*, *Science* **278**, 1432 (1997).
16. B. O. Wells *et al.*, *Science* **277**, 1067 (1997).
17. Y. S. Lee *et al.*, “Neutron Scattering Study of Spin Density Wave Order in the Superconducting State of Excess-Oxygen-Doped $\text{La}_2\text{CuO}_{4+y}$,” cond-mat/9902157.
18. S. Wakimoto *et al.*, “Observation of New Incommensurate Magnetic Correlations at the Lower Critical Concentration for Superconductivity ($x = 0.05$) in $\text{La}_{2-x}\text{Sr}_x\text{CuO}_4$,” cond-mat/9902201.
19. H. A. Mook *et al.*, *Nature* **395**, 580 (1998).
20. J. M. Tranquada, “Charge Stripes and Antiferromagnetism in Insulating Nickelates and Superconducting Cuprates,” cond-mat/9802043; “Experimental Evidence for Topological Doping in the Cuprates,” cond-mat/9903458; J. M. Tranquada, N. Ichikawa, K. Kakurai, and S. Uchida, “Charge Segregation and Antiferromagnetism in High- T_c Superconductors,” cond-mat/9903453.
21. M.-H. Julien *et al.*, “Charge Segregation, Cluster Spin-Glass and Superconductivity in $\text{La}_{1.94}\text{Sr}_{0.06}\text{CuO}_4$,” cond-mat/9903005.
22. A. W. Hunt, P. M. Singer, K. R. Thurber, and T. Imai, “ ^{63}Cu NQR Measurement of Stripe Order Parameter in $\text{La}_{2-x}\text{Sr}_x\text{CuO}_4$,” cond-mat/9902348.
23. P. W. Anderson, *Science* **235**, 1196 (1987).
24. See, for instance, Assa Auerbach, *Interacting Electrons and Quantum Magnetism* (Springer-Verlag, New York, 1994).
25. G. Baskaran and P. W. Anderson, *Phys. Rev. B* **37**, 580 (1988).
26. I. Affleck and J. B. Marston, *Phys. Rev. B* **37**, 3774 (1988).
27. F. D. M. Haldane, “Luttinger’s theorem and bosonization of the Fermi surface,” in *Proceedings of the International School of Physics “Enrico Fermi,” 121 Varenna 1992* edited by R. Schrieffer and R. A. Broglia (North-Holland, New York, NY 1994).
28. J. B. Marston and I. Affleck, *Phys. Rev. B* **39**, 11538 (1989).
29. J. B. Marston, *Phys. Rev. B* **42**, 10804 (1990).
30. I. Affleck, D. P. Arovas, J. B. Marston, and D. A. Rabson, *Nucl. Phys. B* **366**, 467 (1991).
31. G. Kotliar, *Phys. Rev. B* **37**, 3664 (1988).
32. D. Rokhsar, *Phys. Rev. B* **42**, 2526 (1990).
33. R. Laughlin, *Phys. Rev. Lett.* **79**, 1726 (1997); “A Critique of Two Metals,” cond-mat/9709195.

34. J. B. Marston, *Phys. Rev. Lett.* **64**, 1166 (1990).
35. D. H. Kim and P. A. Lee, "Theory of spin excitations in undoped and underdoped cuprates," cond-mat/9810130.
36. Arti Tandon, Ziqian Wang, and Gabriel Kotliar, "Compressibility of the Two-Dimensional Infinite-U Hubbard Model," cond-mat/9904235.
37. T. Hsu, J. B. Marston, and I. Affleck, *Phys. Rev. B* **43**, 2866 (1991).
38. See, for example, J. Zaanen and O. Gunnarsson, *Phys. Rev. B* **40**, 7391 (1989); S. A. Kivelson and V. J. Emery in *The Los Alamos Symposium-1993: Strongly Correlated Electron Systems*, K. S. Bedell *et al.*, eds. (Addison-Wesley, Menlo Park, 1994); V. J. Emery and S. A. Kivelson, *Physica C* **263**, 44 (1996); O. Zachar, S. A. Kivelson and V. J. Emery, *Phys. Rev. B* **57**, 1422 (1995); C. Castellani *et al.*, *Phys. Rev. Lett.* **75**, 4650 (1995); S. White and D. Scalapino, *Phys. Rev. B* **55**, 14701 (1997).
39. T. Tohyama *et al.*, "Stripe Stability in the Extended t-J Model on Planes and Four-Leg Ladders," cond-mat/9809411; Steven R. White and D. J. Scalapino, "Competition Between Stripes and Pairing in a $t - t' - J$ Model," cond-mat/9812187.
40. S. Caprara *et al.*, "The Stripe-Phase Quantum-Critical-Point Scenario for High- T_c Superconductors," cond-mat/9812279; "Single-Particle Properties of a Model for Coexisting Charge and Spin Quasi-Critical Fluctuations Coupled to Electrons," cond-mat/9811130.
41. K. Runge, private communication.
42. Matthew P. A. Fisher, "Mott Insulators, Spin Liquids and Quantum Disordered Superconductivity," cond-mat/9806164.
43. Leon Balents, Matthew P. A. Fisher, and Chetan Nayak, "Nodal Liquid Theory of the Pseudo-Gap Phase of High- T_c Superconductors," cond-mat/9803086; "Dual Order Parameter for the Nodal Liquid," cond-mat/9811236.
44. Leon Balents, Matthew P. A. Fisher, and Chetan Nayak, "Dual Vortex Theory of Strongly Interacting Electrons: A Non-Fermi Liquid with a Twist," cond-mat/9903294.
45. Hyok-Jon Kwon, "Novel Antiferromagnetic Quantum Phase Transition in Underdoped Cuprates," cond-mat/9901208.
46. A. Houghton and J. B. Marston, *Phys. Rev. B* **48**, 7790 (1993).
47. N. Furukawa and T. M. Rice, *J. Phys. Condens. Matter* **10**, L381 (1998).
48. R. Shankar, *Physica A* **177**, 530 (1991); *Rev. Mod. Phys.* **66**, 129 (1994).
49. H.-J. Kwon, *Phys. Rev. B* **55**, 5988 (1997).
50. A. Houghton, J. B. Marston, and H.-J. Kwon, "Multidimensional Bosonization," cond-mat/9810388, to appear in *Advances in Physics*.
51. A. Virosztek and J. Ruvalds, *Phys. Rev. B* **42**, 4064 (1990); J. Ruvalds *et al.*, *Phys. Rev. B* **51**, 3797 (1995).
52. A. T. Zheleznyak, V. M. Yakovenko, and I. E. Dzyaloshinskii, *Phys. Rev. B* **55**, 3200 (1997).
53. Jun-ichiro Kishine and Kenji Yonemitsu, "Anisotropic Suprresion of Quasiparticle Weight in Two-Dimensional Electron System With Partially Flat Fermi Surface: Two-loop Renormalization-group Analysis," cond-mat/9808303.
54. D. Zanchi and H. J. Schulz, "Weakly Correlated Electrons on a Square Lattice: a Renormalization Group Theory," cond-mat/9812303.
55. P. B. Littlewood, and C. M. Varma, *Phys. Rev. B* **46**, 405 (1992); P. B. Littlewood, J. Zaanen, G. Aeppli, H. Monien, *Phys. Rev. B* **48**, 487 (1993).
56. See, for instance, A. J. Millis, H. Monien, and D. Pines, *Phys. Rev. B* **42**, 167 (1990); P. Monthoux, A. V. Balatsky, and D. Pines, *Phys. Rev. Lett.* **67**, 3448 (1991); N. Bulut, D. J. Scalapino, and S. R. White, *Physica C* **246**, 85 (1995).
57. S. C. Zhang, *Science* **275**, 1089 (1997). Also see Eugene Demler and Shou-Cheng Zhang, *Nature* **396**, 733 (1999) and reference therein.